Laser Tuners and Wavelength-Sensitive Detectors Based on Absorbers in Standing Waves

David A. B. Miller, *Senior Member, IEEE*

Abstract—**We propose a new method for making laser tuners and wavelength-sensitive or tunable detectors that is based on absorbers in standing waves. Because the method does not rely on mechanical movement or changes in refractive index, it may offer high-speed tunable devices whose range is not constrained by limits on the size of refractive index changes. The devices can be made either in a longitudinal form by back reflection, or in a transverse form by interfering beams at an angle on a surface. We give theoretical models for these structures, and illustrate the concepts with various specific device designs. These include a narrow band detector based on transverse gratings, a simple wavelength sensitive longitudinal structure with a single absorber, and a two-absorber longitudinal structure capable of many functions, including a narrow band detector, a two-wavelength detector, a wavelength measuring detector, a continuously variable laser tuner, and a laser phase controller. These devices can all be made using layered semiconductor growth and lithography, and are particularly suited to quantum wells. The devices are applicable to wavelength division multiplexing and switching, and to sensors and spectroscopy.**

I. Introduction

THERE is a broad range of applications for tunable lasers and wavelength-sensitive or tunable optical detectors. For example, both can be used in spectroscopy in the laboratory, and for environmental or chemical sensors. The recent growth in interest in optical communications networks has also generated more demand for tunable lasers and detectors for wavelength division multiplexing and switching. Although there are many methods for tuning lasers, it is relatively difficult to make tunable lasers that can be simply controlled, for example with a voltage, and that can be rapidly tuned. There are few simple methods for making tunable or wavelength-sensitive detectors other than combining detectors with conventional optical filters; such filters are also not usually easy to control or tune rapidly. It is particularly difficult to make such lasers and detectors in an integrated form; this difficulty prevents low-cost wavelength-sensitive systems, and inhibits their use in many applications. Here we propose a new approach to both laser tuning and wavelength-sensitive and tunable detectors. This approach is well suited to modern semiconductor technology, and may allow simple and integrable systems.

There are various methods for making detectors sensitive to particular wavelengths, either fixed or tunable. The simplest is to combine the detector with a conventional optical filter (such as a Fabry–Perot resonator [1]) or spectrometer. Such systems are often mechanically set or controlled, such as through the angle of a grating or prism, or the thickness or angle of an interference filter. Another method is to use the wavelength selectivity of some other physical process, as, for example, in the use of surface plasma modes with semiconductor infrared detectors [2]. Other schemes rely on the intrinsic wavelength sensitivity of the absorption process itself, such as the photon energy range of absorption for specific optical transitions. In bulk semiconductors, for example, magnetic field tuning is possible in the far infrared [3]. Recent work on quantum well systems, for example, has utilized the ability to control transition energies through layer thicknesses in growth (see, e.g., [4]), and through the sensitivity of some transitions to electric field (see, e.g., [5]–[9]). Many of these schemes are promising, but they are often restricted to specific spectral regions because they rely on specific physical effects in materials.

Lasers are most simply tuned also by mechanical adjustment of dispersive elements such as gratings, prisms, and filters. Recent work aimed at rapidly tunable lasers for wavelength division multiplexed communications systems uses electrically controlled refractive index to tune the laser in a variety of different schemes (see, e.g., [10]–[15]). These schemes also are promising, but they are all constrained by the difficulty of making large refractive index changes.

We propose here a set of devices based on a different concept. All of them rely on placing absorbing material into a standing wave pattern formed by the interference of waves. This allows two classes of devices, detectors sensitive to specific wavelengths, and absorbers that can be used to set the wavelength of lasers. When additionally the strength of the absorption can be controlled, we can make tunable detectors and tunable lasers. Tunable detectors can also be made by varying the weighting applied to the signals from specific absorbing elements.

The concept of controlling the wavelength of a laser by inserting a thin absorber in standing wave pattern of a laser cavity has been considered before [16], [17]. This technique was used for tuning various lasers [17]. In these previous uses of a thin absorber to tune the laser, the tuning was accomplished by mechanical movement of the position of the absorber. Here we extend this concept to the use of multiple layers of controllable absorption. The idea of periodic structuring of a detector surface to improve coupling of waves or plasmons has also been studied [18], [19], although the concept there is different from the present one of absorbers in standing waves.

Manuscript received April 6, 1993; accepted June 4, 1993, with no revisions.
The author is with AT&T Bell Laboratories, Crawfords Corner Road, Holmdel, NJ 07733-3030 USA.
IEEE Log Number 9215332.

One particular way to control the absorption is through electroabsorptive effects in semiconductors, with quantum wells being well suited to this application. Various of the structures proposed here could, for example, use quantum wells inside p-i-n diodes as electrically controllable absorbers through the quantum-confined Stark effect [20]. The thickness of quantum wells is also well suited to this application; the typical thickness of 10 nm is usually much less than the wavelength of light inside the material, which allows them to "sample" the standing wave field at particular points. For example, quantum wells positioned at standing wave minima will have little or no absorption, as desired for many of the devices. An alternative electroabsorptive mechanism seen in some other semiconductor structures is the Franz-Keldysh effect, which could be used in a similar way to make controllable absorbers. Another possibility is to control the absorption by reducing it through methods often used to emit light, such as injecting current into a forward biased semiconductor diode; the principles discussed here continue to be valid even when the absorption is reduced to the point where it is negative (i.e., where the "absorber" shows gain).

In contrast to many other methods of tuning, there is no mechanical movement of a grating or prism or filtering element required for either the detector or laser tuning. Hence these tunable devices might be both fast and reliable. Since the entire tunable or wavelength-sensitive device could be made as a set of integrated semiconductor diodes, it could also be small and robust.

For the detectors, we are able with this method to make detectors that are sensitive at some wavelengths and less so at others, without relying on the intrinsic wavelength dependence of the absorbing material itself. Thus we may be able to make detectors with, for example, narrow sensitivity ranges, even although the absorbing material itself absorbs over a broad wavelength range. For the lasers, when we use controllable absorbers, the tuning range with this method is limited only by the spectral range over which we can make sufficient changes in absorption.

In this paper, we start in Section II by describing the basic principles of the devices with illustrative examples. In Section III, we distinguish and describe different classes of devices. Section IV presents theoretical models for analyzing the devices. Specific wavelength sensitive detectors are described in Section V, and laser tuning devices are given in Section VI. We summarize the conclusions in Section VII.

II. Basic Principles of the Devices

A. Detectors

To make a wavelength sensitive detector, we construct a set of absorbing regions configured to act as light intensity detectors. An example would be a set of semiconductor photodiodes. We position these detectors within the standing wave pattern formed by interfering two light beams. (Usually we will be interfering two beams formed from one light beam, i.e., interfering a light beam with itself, although there could be some exceptions to this.) Since the relative positions of the standing wave peaks will change as we change wavelength, the relative signals from the different detectors will change, and hence we will have a detection system that is sensitive to wavelength. There are various mathematical ways in which we can compare the detector signals to deduce information about the wavelength or wavelengths present in the light beams, and we will discuss some of these ways below.

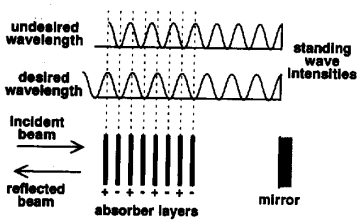

Fig. 1. Layered wavelength-sensitive detector structure. The signals from the absorbing layers are multiplied by the weights shown and then summed in some apparatus not shown. The weights are shown as + for +1 and − for−1. For the desired wavelength, the antinodes in the standing wave pattern formed by reflection of the beam off of the mirror all line up with the absorbing regions with weight of +1, and the nodes line up with the absorbing regions with weight of −1, giving a net summed result of +4. For the specific undesired wavelength shown, the result of the summation is exactly zero. (For simplicity, the mirror is assumed to have no phase change on reflection, so that there will be an antinode in the standing wave pattern at the mirror.)

An example of a detector that is strongly sensitive essentially to only one wavelength is shown in Fig. 1. Here the outputs from a set of detectors are added with the weights shown. At the desired wavelength λ_o, the nodes of the standing wave pattern all line up with the detectors with +1 weighting, whereas the antinodes all line up with the detectors with −1 weighting, so the net detected signal is +4 units. For the case of the other, undesired, wavelength, the net result after the summation in this particular case is zero. In general, only the desired wavelength and some of its harmonics will have no cancellation in the summation. All other wavelengths will experience some cancellation. Hence we have made a wavelength sensitive detector. (For this simple example, we have assumed for simplicity that their is very little absorption in the absorbing regions so that the standing wave pattern is not perturbed by the absorption. We will give a method for analysis below that allows rigorously for the actual absorption.)

Although the specific example in Fig. 1 has the absorbers spaced by quarter wavelengths ($\lambda_o/4$), we can also make devices with other spacings. For example, we could space the absorbers by 3/4 λ_o, and still get identical detected signal at the wavelength λ_o. In general, we can add any integer number of half wavelengths to the spacing, and still get the same detected signal at λ_o, although the wavelength sensitivity of the detector will be changed and the detector will now also detect some other wavelengths. This option to space the absorbers further apart may be useful for fabrication of some devices where it is difficult to put the layers very close together; for example, it could be difficult to contact separate detectors if they are only spaced $\lambda_o/4$ apart.

We can also imagine devices where we could vary, or even turn off or on, the absorption in particular layers so that we could tune the wavelength at which the detector was sensitive. The use of other weighting factors in the sensing of the

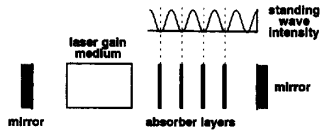

Fig. 2. Example configuration using a layered structure with absorbers to control the wavelength of a laser. The laser is shown running at a wavelength such that the standing wave pattern has minima at the positions of the absorbers in the cavity. The laser will tend to select wavelengths that minimize loss. (For simplicity, the mirror is assumed to have no phase change on reflection, so that there will be an antinode in the standing wave pattern at the mirror.)

detector output could also be used to change the wavelength sensitivity of the system overall.

It would also be possible in principle to make controllable detectors involving negative absorption (gain), since the resulting stimulated emission would in principle alter the current flowing in, for example, a forward biased diode. Such current changes would, however, likely be small compared to the existing forward current in such a forward-biased diode, and hence the signal might be small compared to the noise (e.g., shot noise).

B. Laser Tuners

To tune a laser using absorbers, we position absorbers at appropriate points in a standing wave pattern in the laser cavity. The laser will tend to run at the wavelength that gives lowest loss (or, to be more correct, the largest difference between gain and loss). Fig. 2 shows a simple case where a structure with layered absorbers is placed near the end mirror of a laser cavity. In this case, the laser will tend to run at a wavelength λ_o that gives antinodes at the positions of the absorbers, hence minimizing absorption.

As with other methods of tuning lasers, the laser chooses the lowest loss mode because this mode will grow faster than the other modes, and hence will tend to become dominant. Eventually, this power in this dominant mode will tend to reduce the laser gain by saturating it, and this mode will have gain equal to loss overall. All the other modes, which have less gain to start with, will tend therefore to have gain less than loss, and cannot therefore grow—in fact, they will tend to die out.

Just as for the detectors, we could add integer numbers of half wavelengths (i.e., $\lambda_o/2$) of spacing between the absorbers while still retaining low loss at wavelength λ_o. Again, this would allow low loss at some other wavelengths also.

We could also imagine a version of a structure like that of Fig. 2 in which, rather than having absorbing regions, we had gain regions (i.e., regions of negative absorption). The laser would then tend to run at a wavelength for which the antinodes of the standing wave pattern coincided with the gain regions. We could further extend this to have both positive and negative absorbers, with the laser then trying to run with nodes at the (positive) absorbers and antinodes at the gain (negative absorption) regions.

By controlling the absorption (positive or negative) in particular layers, we can clearly control the wavelength at which the structure has minimum loss (or, equivalently, maximum gain), and hence we can control the laser wavelength.

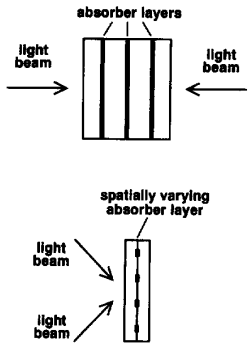

Fig. 3. Two types of structure for the devices. (a) Longitudinal grating device, with beams shown counterpropagating. A standing wave pattern will be formed with the absorbing layers coinciding with specific parts of the standing wave pattern. (b) Transverse grating device, with beams shown propagating at an angle. A standing wave pattern will be formed in which the intensity will vary laterally within the absorbing layer. In this case, the absorption within the absorbing layer will be different at different positions in the layer, with stronger absorption chosen to coincide with specific parts of the standing wave pattern.

III. Classes of Device Structures

In the way that the devices are made, we can distinguish two general classes. One class is based on longitudinal interference patterns, in which the layers in a multiple layered structure are designed to coincide with particular points in a standing wave pattern. This first class would typically involve two counterpropagating beams propagating perpendicular to the surface (although the beams need not necessarily be counterpropagating, nor need they be perpendicular to the surface). The second class is based on transverse interference patterns, in which different points on a surface correspond to different points on a standing wave pattern. In this second class, the standing wave pattern would typically be formed by two beams at an angle to each other incident on a plane surface, although neither the angle or planarity of the surface are necessary restrictions. This second method allows larger spacing of the nodes and antinodes, which may allow complex structures of absorbers to be fabricated by conventional lithography. It may also be easier with the transverse grating structure to make separate connections to each of the absorbing regions using standard lithographic techniques. For both classes of devices, it is necessary that a standing wave pattern be formed. These general classes are illustrated in Fig. 3.

IV. Theory of Absorption by Absorbing Gratings

A. Longitudinal Gratings

Simple Theory—Standing Wave Patterns Neglecting Loss: The simplest theory of such absorbing gratings is one where we neglect the absorption within the absorbing layers when we calculate the standing wave pattern. Hence this is a weak absorption theory, accurate in the limit of very small absorption. In such a theory, we first calculate the standing

wave pattern neglecting any loss, and then calculate the total absorption based on that standing wave pattern within the absorbers. This is implicitly the simplifying assumption we used in the discussions above to illustrate the basic ideas. In the very simplest applications of it we might also further simplify by assuming the same refractive index in the absorbing and nonabsorbing layers, and neglecting any reflection due to the absorbing nature of the layers. (There is always some reflection off of an absorbing material, regardless of its refractive index.) This is the approach we will take in this paper when using this simple theory.

To illustrate this model with the simplest example, for a 100% reflecting mirror, with no phase change on reflection off of the mirror, the standing wave intensity pattern for a monochromatic wave of wavevector k in the positive z direction (i.e., corresponding to propagation to the right in Figs. 1 and 2) is

$$I(z) = 2I_0(1 + \cos 2kz) \tag{4.A.1}$$

where we have chosen $z = 0$ at the position of the mirror. For zero phase change on reflection, an antinode occurs at the mirror surface. For illustrative purposes in this paper, we will typically use a such hypothetical mirror with 100% reflection and no phase change on reflection. It is straightforward to extend this theory to include both phase shift on reflection [which will add a phase angle in the cosine term of (4.A.1)] and other reflectivities (which will change the depth of the standing wave pattern). Wavelength-dependent phase shifts, common in many mirrors, could also be straightforwardly included.

This simple theory allows some simple analytic results, and gives a useful first approximation. One application of this theory is to calculate to a first approximation the loss when we put an absorber of finite thickness at a node in a standing wave pattern. This is particularly relevant for the case of the laser tuner, since this will be a common operating mode. Such a calculation will tell us how thick we can make the absorbing layers in practice without incurring excessive loss in the "low-loss" condition. For this particular case, this simple theory will be a good approximation because it is analyzing a case where there is little or no loss anyway.

Let us presume we have an absorbing layer, of absorption coefficient α and thickness b. We will also presume it to be much less than an absorption length in thickness, i.e., $b \gg 1/\alpha$, so that the total absorption for a unidirectional beam propagating through the layer would be $A = \alpha b$. For an absorber centered at position z_b, the actual loss in the standing wave will be

$$\begin{aligned} L &= 2\alpha \int_{z_b - b/2}^{z_b + b/2} (1 + \cos 2kz)dz \\ &= 2\alpha \left[b + \frac{1}{k} \sin kb \cos 2kz_b \right]. \end{aligned} \tag{4.A.2}$$

We can see that, for an absorber positioned exactly at an antinode ($\cos 2kz_b = +1$ in this case), the absorption is 4 A. The factor of 4 comes from two factors of 2, one of which is due to the fact that we have beams of unit intensity propagating in *both* directions (so that the average overall intensity is 2 units), and the other factor of 2 comes from the standing wave effect. This relation, (4.A.2), is plotted in dimensionless units in Fig. 4 for the case of an absorber centered exactly at a node (in this case, $\cos 2kz_b = -1$).

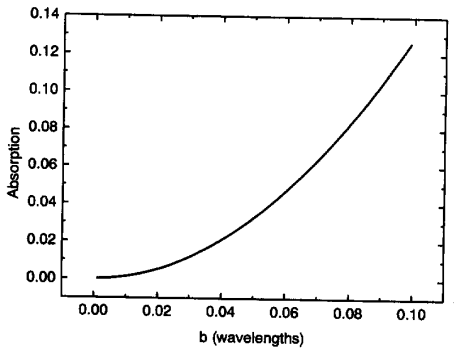

Fig. 4. Absorption for a thin absorber centered at a node, as a function of the thickness, b, of the absorber. Absorption is in units of the absorption of the layer for a unidirectional beam (i.e., in units of $A = \alpha b$). Thickness is in units of wavelengths (inside the material), for the case of a longitudinal grating. For a transverse grating, the unit of b is the "wavelength" of the interference pattern, which is twice the repeat distance of the intensity interference pattern (i.e., $2\Delta x$) and the absorptions are given for the "two-beam" interference case.

When the absorber is exactly centered on a node, the resulting absorption is, to lowest order in k,

$$L_{\text{node}} = \frac{\alpha k^2 b^3}{3} = \frac{4\pi^2}{3} \frac{\alpha b^3}{\lambda^2}. \tag{4.A.3}$$

where λ is the wavelength.

For example, for a medium of refractive index 3.5, with an absorbing layer thickness of 10 nm, and a (free-space) wavelength of 850 nm (numbers appropriate for a GaAs quantum well as the absorber in an otherwise AlGaAs structure), the absorber is approximately 0.041 wavelengths thick (measured in wavelengths *inside* the material), and the actual absorption in the layer at the node will be $L_{\text{node}} \cong 0.022A$, where $A = \alpha b$ would be the single-pass loss for a unidirectional beam passing through the same absorber. This calculation illustrates that such quantum wells would be well suited to such longitudinal structures; they would be thin enough that they would have very little absorption when placed at a node.

B. Full Theory Including Loss

General Method of Solution: The simple method discussed above is clearly not self-consistent. We are first calculating the standing wave pattern neglecting absorption, and then calculating the absorption without including its effect on the standing wave pattern. The proper, general way to solve this problem is simply to solve the wave equation using the appropriate boundary conditions. For example, for the case of a monochromatic standing wave formed by retro-reflection off a 100% mirror with no phase change on reflection, the boundary condition is that the derivative of the wave amplitude is zero at the mirror, and the forward and backward waves have equal amplitudes. This problem could now be solved by starting at the mirror, and working backwards (i.e., integrating) through the structure. (The amplitude at the mirror can be chosen arbitrarily initially, and fixed at the end of the problem based

on, for example, the known incident intensity.) The different absorptions and refractive indices in the structure could be formally included using a spatially-varying dielectric constant in the integration.

It is clear also that we could extend this technique to include the case of any particular finite reflectivity of the end mirror, and any phase change on reflection. In this case, the forward and backward waves would have different (complex) amplitudes, but we would still know the amplitude at the mirror, and could still deduce the derivative at the mirror. With such finite reflectivity, we could impose the condition of a particular amplitude transmitted by the mirror, and no wave incident from the external side of the mirror. These would be sufficient conditions to determine the amplitude and field derivative at the inside of the mirror.

We will be most interested in the solutions in the case of a multiple layered structure, in each layer of which the absorption and refractive index are constant. In this case, we can obtain the exact, general solution for a given layer, and obtain the solution for the entire structure using matrix techniques.

The method of solution of such problems is well known in the theory of multilayer dielectric interference filters (see, e.g., Macleod [21]). We presume normal incidence with a plane wave in an isotropic, nonmagnetic medium. The incident wave is monochromatic with angular frequency ω, so at any point in the structure, the wave is of the form

$$E = \frac{1}{2}E_0 e^{i\omega t} + c.c. \tag{4.A.4}$$

Hence, the wave equation can be written in the form

$$\frac{d^2E_0}{dz^2} = -\left[\frac{n^2\omega^2}{c^2} - \frac{\alpha^2}{4} - i\frac{n\alpha\omega}{c}\right]E_0 \tag{4.A.5}$$

for a particular uniform layer, where we have anticipated a convenient notation for the general solution,

$$E_0(z) = Fe^{-i\left(k-i\frac{\alpha}{2}\right)z} + Be^{i\left(k-i\frac{\alpha}{2}\right)z}. \tag{4.A.6}$$

In (4.A.5) and (4.A.6), the symbols have the usual meanings: n is the refractive index, α is the absorption coefficient, c is the velocity of light in free space, and the wave vector $k = 2\pi n/\lambda$ (where λ is the free space wavelength). F is the amplitude of the forward-going wave and B is the amplitude of the backward-going wave. F and B are in general complex. Note that this sum of forward and backward waves is a general solution for (4.A.5) for a uniform layer, and allows matching of amplitude and derivative at a boundary.

At a given interface between two layers of different materials, the boundary conditions are continuity of the transverse component of the electric field, which here means continuity of E_0, and continuity of the transverse component of the magnetic field, which here results in continuity of dE_0/dz. Simple algebra then gives the relations between the wave amplitudes on the "left" of a boundary (F_L and B_L) and those on the "right" (F_R and B_R)

$$F_L = \frac{1}{2}[F_R(1+\sigma) + B_R(1-\sigma)] \tag{4.A.7}$$

$$B_L = \frac{1}{2}[F_R(1-\sigma) + B_R(1+\sigma)] \tag{4.A.8}$$

where

$$\sigma = \frac{ik_R + \alpha_R/2}{ik_L + \alpha_L/2}, \tag{4.A.9}$$

in which the subscripts L and R refer to the materials on the left and right of the boundary respectively.

We can conveniently write (4.A.7) and (4.A.8) in matrix form. We will define a column vector

$$S = \begin{bmatrix} F \\ B \end{bmatrix} \tag{4.A.10}$$

whose elements are the forward and backward wave amplitudes. (Our matrix formulation differs from, e.g., [21] by using forward and backward amplitudes rather than amplitude and derivative, but these are both valid mathematically.) Then we can write

$$S_L = DS_R \tag{4.A.11}$$

(where S_L and S_R refer to the amplitude vectors on the left and right of the boundary respectively), in which

$$D = \begin{bmatrix} \frac{(1+\sigma)}{2} & \frac{(1-\sigma)}{2} \\ \frac{(1-\sigma)}{2} & \frac{(1+\sigma)}{2} \end{bmatrix}. \tag{4.A.12}$$

Using the same conventions, we can also define a propagation matrix, P, that relates the wave amplitude vector just inside the right hand side of a layer to those just inside the left side of the same layer,

$$P = \begin{bmatrix} e^{i(k-i\alpha/2)l} & 0 \\ 0 & e^{-i(k-i\alpha/2)l} \end{bmatrix}, \tag{4.A.13}$$

where l is the thickness of the layer. Hence we can relate the wave amplitude vector, S_1, just inside the right hand side of the right-most layer (e.g., at the mirror surface), to the wave amplitude vector just to the left of the left-most layer of an m layer structure (e.g., the entrance face of the whole structure) through the matrix multiplication

$$S_{n+1} = \left[\prod_m D_m P_m\right] S_0 \tag{4.A.14}$$

where we multiply to the left with increasing m. (The $m+1$ th layer is the material to the left of the whole structure; only its absorption and refractive index are needed, not its thickness.)

Hence we have a complete formalism for calculating the standing wave and its absorption for an arbitrary layered structure. Incidentally, for the case of a mirror that is itself a dielectric stack, we can include the calculation of the mirror reflectivity into the model. A particularly useful consequence of this is that we can then implicitly include the change in phase with wavelength for reflection off of such a mirror. For dielectric stack mirrors, the phase change on reflection can change quite markedly with wavelength. When the mirror layer structure is included in the calculation, a convenient form for the vector S for the right-most interface is to choose it to have unit forward amplitude and zero backward amplitude just to the right of the right-most interface. This means we are presuming a wave "leaks" through the mirror, but that no wave is incident from the right. The overall reflectivity of

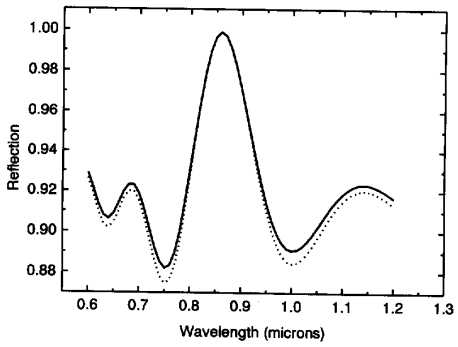

Fig. 5. Comparison of the exact theory (solid line), obtained by solving the wave equation, and the approximate theory (dotted line), obtained by calculating the standing wave pattern neglecting absorption, and then evaluating the absorption based on this standing wave. The structure calculated contained four 10 nm thick layers of absorption coefficient 1 μm^{-1}, separated by nonabsorbing layers 0.1114 μm thick, with this whole structure separated by a nonabsorbing layer 0.1821 μm thick from a 100% reflecting mirror with no phase change on reflection. All layers have refractive index of 3.5, and the wave enters through a similar nonabsorbing medium (to avoid front surface reflection). At 850 nm, these thicknesses correspond to $\lambda/2$ optical thickness between the centers of the absorbing layers, and a $3\lambda/4$ spacing of the first absorbing layer from the mirror. This is essentially the structure shown for the absorber and mirror in Fig. 2.

the structure can be deduced as before from the ratio of the forward and backward amplitudes in the vector S just to the left of the left-most interface.

The two methods, approximate and exact, are compared in the calculation shown in Fig. 5, which is based on a structure like that of absorber and mirror in Fig. 2.

Fig. 5 shows that, at least for this relatively low absorption structure, the exact and approximate calculations are similar. Note that the exact solution gives more reflection at the minima, presumably because the standing wave pattern is less strong when absorption is included (the forward and backward waves no longer have equal amplitude).

Explicit Calculation of Absorption in a Layer: For detectors in particular, it is useful to know how much absorption there is in a given layer. The results presented above do correctly give the reflectivity or transmissivity of the structure as a whole, but do not explicitly give the amount of absorption in a given layer. We can obtain this absorption from this formalism, as we will derive here.

Formally, we write the polarization P induced by the electric field E as

$$P = Kd \tag{4.A.15}$$

where d is the induced dipole moment per unit volume, and K is a dimensioning constant that depends on the system of units. We presume that the material is linear and isotropic, so that d and P are in the same direction as E and are linearly proportional to E. The work done by the field E on the material per unit volume is therefore

$$W = \frac{1}{K}\int E\frac{dP}{dt}dt \tag{4.A.16}$$

where t represents time. After averaging over one cycle of the field, we obtain

$$\frac{dW}{dt} = \frac{n\alpha c}{2K}|E_0|^2 \tag{4.A.17}$$

which is the absorbed power per unit volume.

For a given uniform layer, j, we can integrate this over the thickness of the layer, l_j, to find the absorbed power per unit area, $I_{\mathrm{abs}j}$. It will be convenient for calculations to define the absorbed power in terms of the forward and backward wave amplitudes, $F_{\mathrm{RHS}j}$ and $B_{\mathrm{RHS}j}$, just inside the right hand side of the layer. The result of the integration, based on the solution (4.A.6), is, for layer j,

$$I_{\mathrm{abs}j} = \frac{n_j\alpha_j c}{2K}G_j \tag{4.A.18}$$

where

$$\begin{aligned} G_j = \frac{1}{\alpha_j}\Big[&|F_{\mathrm{RHS}j}|^2(\exp\{\alpha_j l_j\} - 1) \\ &+ |B_{\mathrm{RHS}j}|^2(1 - \exp\{-\alpha_j l_j\})\Big] \\ &+ \frac{1}{k_j}\big[\mathrm{Re}\big(F_{\mathrm{RHS}j}B^*_{\mathrm{RHS}j}\big)\sin(2k_j l_j) \\ &+ \mathrm{Im}\big(F_{\mathrm{RHS}j}B^*_{\mathrm{RHS}j}\big)\{\cos(2k_j l_j) - 1\}\big] \end{aligned} \tag{4.A.19}$$

where k_j and α_j are the wavevector and absorption coefficient respectively for layer j.

The intensity, I_{inc}, incident on the whole structure (i.e., the intensity in the material to the left of the whole structure, formally, layer $m+1$) is given by

$$I_{\mathrm{inc}} = \frac{n_{m+1}c}{2K}|F_{\mathrm{RHS}m+1}|^2. \tag{4.A.20}$$

Hence, the fraction of the incident power absorbed in layer j is given by

$$\frac{I_{\mathrm{abs}j}}{I_{\mathrm{inc}}} = \frac{n_j}{n_{m+1}}\alpha_j\frac{G_i}{|F_{\mathrm{RHS}m+1}|^2}. \tag{4.A.21}$$

Therefore, once the whole problem is solved for the field amplitudes at each interface using the exact method discussed in the previous section, we can deduce the fraction of the incident power absorbed in each layer using relation (4.A.21).

Qualitative Effects of Finite Absorption: Note that in general the effect of finite absorption is to reduce the spectral selectivity of the structure compared to the case of vanishingly small absorption in the absorbing layers. By spectral selectivity here, we mean the ratio of the absorption at one desired wavelength to that at an undesired wavelength. Of course, the finite absorption case will have larger total absorption *difference* between the two wavelengths. The reason it will have less selectivity is because, as the finite absorption becomes stronger, the reflected wave from the structure overall becomes weaker. As a result, the relative depth of the standing wave will become weaker as we move away from the mirror through the absorbing layers. In a strongly absorbing structure, there would be little standing wave at all near the beginning of the structure (i.e., the end where the wave enters the structure). There would, however, be a relatively strong average intensity from the forward propagating wave, which would give rise to absorption that was essentially independent of wavelength.

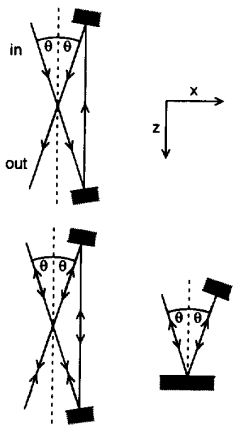

Fig. 6. Beam paths forming transverse interference patterns in the regions where the beams cross. (a) involves only two beam paths in the interference. (b) and (c) have counterpropagating beams, and a total of four beam paths are involved in the interference.

B. Transverse Gratings

For the case of transverse gratings, we will only attempt a simple theory in which the standing wave pattern is calculated neglecting the loss in the absorber. We will also neglect any refractive index variations within the layers containing the absorbing medium. Any full theory including such absorption or refraction variations would require solving a full wave problem in two or even three dimensions. Various effects would have to be included in such a full theory. For example, we would need to include all of the diffraction effects of a wave interacting with a spatially varying absorber or refractive index. We can, however, reasonably imagine that such a simple theory will give a good approximation as long as there is not much absorption from the wave as it passes through the absorbing material nor strong refractive index differences between absorbing and nonabsorbing parts of the material.

Simple Theory—Relative Absorption Neglecting Loss To model transverse gratings in this simple model, we must first understand the form of the interference patterns. Fig. 6 illustrates various configurations for interfering beams to form lateral interference patterns. There are two general classes: in one class, the "two beam" class, only two versions of the beam are involved in the interference; in the second, "four beam" class, there are two beam directions, each with a counterpropagating version.

In the "two-beam" case (case (a) of Fig. 6), only a transverse interference pattern is formed. In the "four-beam" case, there is also a longitudinal interference pattern (i.e., an interference pattern in the direction of the dashed line in Fig. 6). The distinction between the two-beam and four-beam cases is important for two reasons: (i) in the four-beam case, the position of the absorbers in the longitudinal direction is important; (ii) the peak intensity is larger in the four-beam case because of the additional interference, giving rise to more absorption for an absorber placed at the peak. In the four-beam case, it is not necessary that the two pairs of beams be exactly counterpropagating, although for simplicity this is the only case we will analyze here. It is also the case that is relevant for a laser tuner in a linear cavity.

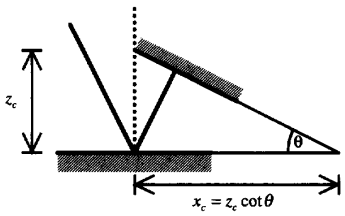

Fig. 7. Geometry of transverse grating mirrors.

To understand the lateral and longitudinal interference patterns, we can formally evaluate the electric field and the intensity in each case. We take a monochromatic field of the general form given in (4.A.4), but with an explicit k-vector. The incoming beam in Fig. 6(a) is then of the form

$$E(z) = \frac{1}{2}E_0 e^{i(\omega t - \mathbf{k}\cdot\mathbf{r})} + c.c. \tag{4.B.1}$$

where

$$\mathbf{k} = \hat{\mathbf{x}}k\sin\theta + \hat{\mathbf{z}}\cos\theta. \tag{4.B.2}$$

With this choice of field, the standing wave intensity pattern (essentially the time-averaged squared modulus of the electric field) becomes

$$I_{\mathrm{TOT}}(x,z) = 2I_0[1+\cos(2kx\sin\theta)] \tag{4.B.3}$$

for the two-beam case, and

$$I_{\mathrm{TOT}}(x,z) = 4I_0[1+\cos(2kx\sin\theta)][1+\cos(2kz\cos\theta)] \tag{4.B.4}$$

for the four-beam case. In both expressions, I_0 is the incident intensity in one beam.

In both the two-beam and four-beam cases in the configurations in Fig. 6, the origin for x is conveniently chosen at the point where the two reflecting surfaces meet. This point is analogous to the position of the mirror in the longitudinal grating case ($z = 0$) in the examples of Figs. 1 and 2, and the standing wave pattern of (4.A.1). Fig. 7 illustrates the distances for the transverse case. Although shown explicitly only for the case (c), the intersection distance x_c is the same for the cases (a) and (b) of Fig. 6.

For the two-beam case, the interference pattern is independent of z (within the intersection region of the beams), and is parallel to the z-axis. For the four-beam case, the interference pattern is the product of a transverse pattern (just like the two-beam case) and a longitudinal pattern. In the four-beam case, if we are using absorbers thin compared to a wavelength in the material, this additional longitudinal interference pattern will affect where we position the absorbers; thin absorbers should be positioned (in the z-direction) near to the position of the peak of the longitudinal standing wave pattern if we are trying to utilize the transverse grating either for laser tuning or wavelength sensitive detection. (Of course, it is also possible instead to use the *longitudinal* grating for the tuning or detection in this four-beam configuration, in which case the absorbers should be positioned (in the x-direction) near

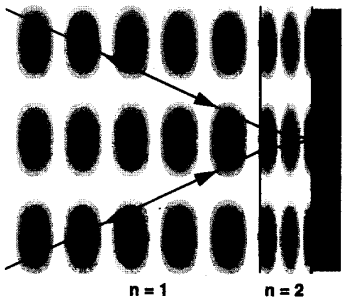

Fig. 8. Illustration of the standing wave pattern for the case of "four-beam" interference, in this case due to counterpropagating beams reflecting off the mirror at the right. Darker regions correspond to higher intensity in the standing wave pattern. This figure also shows the transition between two materials of different refractive index. Although the angles of the beams are changed in passing between the two materials, the spacing of the *transverse* interference pattern is not changed; the spacing of the longitudinal pattern does change, however, as shown. For simplicity, this figure implicitly assumes that there is no reflection off of the interface, which can be arranged in practice with an antireflection coating (not shown). For this illustration, the beams are incident at an angle of 25° to the normal to the surfaces, and the two media have refractive indices of 1 and 2 as shown. The medium of index $n = 2$ has a thickness of 0.6 free-space wavelengths in this illustration. The mirror is presumed to have zero phase change on reflection.

the peaks of the *transverse* interference pattern.) Of course, if the absorbers are much thicker than the wavelength in the material, the positioning in the z-direction is not critical. Fig. 8 illustrates the form of the standing wave pattern in the four-beam case.

This sensitivity to the position of the longitudinal maxima in the interference pattern in the four-beam case means, for example, that the phase change on reflection from the lower mirror in the configuration of Fig. 6(c) (or the mirror in Fig. 8) is important. This phase change will affect the optimum positioning of thin absorber layers in the z-direction relative to the mirror.

The factors of 2 and 4 respectively in (4.B.3) and (4.B.4) arise simply from the number of beams. The peak value of a bracketed term in these equations is clearly 2, and is the result of the interference. In the two-beam case, the resulting peak value of I_{TOT} is $4I_0$, whereas in the four-beam case the peak value of I_{TOT} is $16I_0$. Hence the absorption for an absorber placed at a peak in the interference pattern in the four-beam case is 16 times larger than that for the same absorbing material in a single beam.

In both the two-beam and four-beam cases, the spacing between maxima (or minima) in the interference pattern in the x-direction is

$$\Delta x = \frac{\lambda}{2n \sin \theta}, \tag{4.B.5}$$

where λ is the free-space wavelength, and n is the refractive index of the medium. Because $\sin\theta$ can be small for small angles θ, we can obtain a much larger separation of the minima or maxima than in the longitudinal grating case. This larger separation is one of the advantages of the transverse gratings, since it is difficult to fabricate some kinds of patterns of absorbers if all of the separations are of the order of a wavelength of light; this is especially true if we wish to make electrical contacts to each of the absorbers.

In the four-beam case, the longitudinal interference pattern has a spacing of minima or maxima of

$$\Delta z = \frac{\lambda}{2n \cos \theta}. \tag{4.B.6}$$

Since θ is likely to be small in such designs, Δz is likely to be about half of the wavelength in the material, just as for the longitudinal grating configurations.

It will frequently be the case that the absorber will have a different refractive index (or will be imbedded in a material of different refractive index) from the medium in which the beam is incident. This situation is sketched in Fig. 8. Note that the spacing of the transverse interference maxima or minima does not change through the interface. This is a simple consequence of Snell's law of refraction; the product of refractive index and the sine of the incidence angle is the same on both sides of the interface, and so the denominator in (4.B.5) does not change.

The specific configurations of Fig. 6 are suited for particular applications. The situation in Fig. 6(a) could be used for tuning a unidirectional ring laser, or for a wavelength sensitive detector with the useful property that the power not absorbed in one detector could be transmitted to a following detector. This property could be particularly useful for separately detecting signals at several different wavelengths in the same beam. For the case of the simple longitudinal grating detectors, we would have to separate the incident and reflected beams to "chain" such detectors.

The situation of Fig. 6(b) is suitable for a laser tuner in a bidirectional ring laser cavity, or as a tuner inserted into a linear laser cavity (i.e., where the tuner is not functioning as the cavity end mirror). The case of Fig. 6(c) is suited for a variety of wavelength sensitive detectors and for tuning with a linear laser cavity (where the tuner is one of the cavity end mirrors).

The theory given in section (4.A.1) above for the loss for a finite thickness of absorber translates directly to the two-beam transverse grating case. Instead of comparing the thickness of the absorber to the wavelength, we instead compare the lateral width, w, of the absorber to the repeat distance of the transverse interference pattern. Explicitly, the relevant parameter in Fig. 4 is now $b = w/2\Delta x$. This model also works for the four-beam case, except that the absolute absorption levels may be different because of the four beams and the positioning of the absorbers in the longitudinal interference pattern. Fig. 4 can still be used to deduce the relative absorption of an absorber at a node compared to an absorber at an antinode. (Remember that the units in Fig. 4 are such that the absorption at an antinode is 4 units).

One of the main advantages of this transverse configuration is that the separation of the absorbers can be much larger than the wavelength, hence allowing standard lithographic techniques to be used to pattern absorbers on a surface. For example, from (4.B.5), for a separation between minima of $\Delta x = 10\ \mu$m at a wavelength of 850 nm, the angle of incidence should be $\theta = 2.44°$. Such a separation would allow lithographic fabrication using existing techniques. For

an absorber width of $w = 1$ μm, the parameter b of Fig. 4 is $b = 1/20$. Hence, the ratio of the absorption at a node to absorption at an antinode for this absorber width of 1 μm would be approximately 0.008. Even for an absorber width of 2 μm, this ratio is still only about 3%. Since widths of 1 μm are well within the capabilities of present lithography, these numbers illustrate that we could fabricate transverse absorption grating structures with good wavelength-selective behavior.

V. Wavelength-Sensitive Detection

A. General Method of Detecting a Particular Frequency of Wave

An important general result, obtained using the simple theory that neglects the absorption when calculating the standing wave pattern, is that we can detect any particular spectral component in a wave by an appropriate choice of the weights in a multiple detector structure, in either longitudinal or transverse configuration. As we will show below, to detect a wave of wavevector k, we use a set of weights for the detector sensitivities (both positive and negative) that are given by a (co)sine wave of wavevector $2k$. This method can be used with both longitudinal and transverse grating structures. We will derive the theory using the terminology of the longitudinal grating structure. One very important feature of such a detector is that the desired wavelength to be detected can be chosen electronically by controlling the weights applied to the detector outputs when summing them (or by controlling the amount of absorption in the detectors).

This theory is approximate; it makes a number of simplifying mathematical assumptions. It does, however, indicate the kinds of structures that can be expected to be useful for detecting particular wavelengths. Of course, for any particular structure, the theory presented above can be used to give an accurate calculation for that structure, especially for the longitudinal grating structures where we have a complete absorption theory.

Suppose that we have an incident plane wave electric field that is made up of components at different frequencies. Formally we can write this as

$$E_{\text{inc}}(z,t) = \frac{1}{2}\int_0^\infty E_{\text{inc}}(\omega)e^{i(\omega t - kz)}d\omega + c.c. \qquad (5.A.1)$$

Here k is the wavevector inside the material ($k = n\omega/c$), and the material is assumed to have a uniform refractive index. Because we are using the simple model here, the wave at each point z is calculated neglecting the absorption in the structure.

Now we add to this field a reflected (or counterpropagating) version of itself. For simplicity here, we will assume 100% reflection, with no phase change on reflection, at a position $z = 0$. None of these are necessary restrictions, and the model here may easily be extended to change any of these assumptions. Changing the amount of reflection changes the depth of the standing wave pattern; this device concept works best with 100% reflection. Changing the phase change on reflection or the mirror position merely changes the position of the standing wave pattern in the z direction. The resulting total field is

$$E_{\text{TOT}}(z,t) = \int_0^\infty E_{\text{inc}}(\omega)e^{i\omega t}\cos\left(\frac{n\omega}{c}z\right)d\omega + c.c. \quad (5.A.2)$$

In operation, we will be using detectors sensitive to intensity, not field. Within a given material, intensity is proportional to the square of the modulus of the electric field. For this device concept, we will presume that the detectors integrate in time over a time long compared to the optical cycle, or even long compared to the "beat frequency" of any two frequencies we wish to distinguish. Hence, the integration time is essentially infinite as far as the optical frequencies are concerned; this allows us formally to use infinite limits in our mathematical integration. The time-integrated signal, $D(z)$, in a given detector at a position z will be proportional to the total fluence, $J_{\text{TOT}}(z)$, (i.e., to the time integral of the squared modulus of the electric field) at position z. Hence we have

$$D(z) \propto J_{\text{TOT}}(z) \propto \int_{-\infty}^\infty |E_{\text{TOT}}(z,t)|^2 dt. \qquad (5.A.3)$$

In performing the time integral, we neglect high-frequency oscillating terms in the result as usual, and formally restrict our results to non-zero frequencies. The result is

$$J_{\text{TOT}}(z) = 4\pi\int_0^\infty I_{\text{inc}}(\omega)\left[1 + \cos\left(2\frac{n\omega}{c}z\right)\right]d\omega, \quad (5.A.4)$$

where $I_{\text{inc}}(\omega)$ is the incident intensity at frequency ω. This result states essentially that the time-averaged standing wave pattern is simply the sum of the standing wave patterns of the individual frequency components; all of the interferences between the different frequency components average to zero in the time integration.

It is now straightforward in principle to measure the incident intensity at any particular frequency if we have an appropriate set of detectors sampling different points in the standing wave pattern. The simplest case to analyze, although somewhat difficult to realize physically, is the case where we have some continuous set of detectors, so that we may sample all points within some range of z between $z_{\min}$ and $z_{\max}$. The signal, $D(z)$, from the detector at position z will be multiplied by the value of some weighting function, $U(z)$, and all of the results will be summed to give a result S, i.e.,

$$S = \int_{z_{\min}}^{z_{\max}} D(z)U(z)dz. \qquad (5.A.5)$$

We put one restriction on $U(z)$, which is that it averages to zero within the range $z_{\min}$ to $z_{\max}$, i.e.,

$$\int_{z_{\min}}^{z_{\max}} U(z)dz = 0. \qquad (5.A.6)$$

This restriction is so that we do not get a net signal from the "d.c. level" average intensity in the standing wave pattern. With this restriction, we have formally

$$S \propto 4\pi\int_{\omega=0}^\infty I_{\text{inc}}(\omega)F(\omega)d\omega \qquad (5.A.7)$$

where

$$F(\omega) = \int_{z=z_{\min}}^{z_{\max}} U(z) \cos\left(2\frac{n\omega}{c}z\right) dz. \tag{5.A.8}$$

If we now choose

$$U(z) = \cos 2k'z, \tag{5.A.9}$$

formally evaluating F, we obtain

$$F(\omega) = \frac{1}{2}\left[\frac{\sin(2[k-k']z_{\max})}{2[k-k']} - \frac{\sin(2[k-k']z_{\min})}{2[k-k']}\right] \tag{5.A.10}$$

where we have neglected the terms of order $1/(k' + n\omega/c)$ since these will be negligibly small by comparison. For the simple case of $z_{\min} = -z_{\max}$, we have

$$F(\omega) = \frac{\sin(2[k-k']z_{\max})}{2[k-k']}, \tag{5.A.11}$$

and for the other simple case of $z_{\min} = 0$, the result is half of that in (5.A.11); hence, in these two simple cases, we acquire the common "$\sin(f)/f$" resolution function. In the limit that the integration limits extend to infinity, we get the result

$$S \propto I_{\text{inc}}(\omega = k'c/n). \tag{5.A.12}$$

In other words, we will have measured the strength of the component of the incident signal at a particular frequency. For finite integration limits $z_{\min} = -z_{\max}$ or $z_{\min} = 0$, round about the particular frequency we will have a finite resolution width of the order of

$$\delta\omega \cong \frac{\pi c}{n z_{\max}}, \tag{5.A.13}$$

where we have taken $\delta\omega$ to correspond to the distance between the first zeros of F on either side of the maximum (i.e., a full width to first zero).

In practice, we will not have the desired continuous function $U(z)$, but rather a sampled version of it, because we will have a set of thin absorbers sampling the standing wave at a set of points. We can, of course, use our theories above to calculate the exact result for any particular set of absorbers. One simple and useful case is where we have a uniformly spaced set of similar thin absorbers, spaced with a period d_o, and of thickness h. We then formally have a "sampling function"

$$\begin{aligned} G(z) &= 1 \quad z_o + md_o - \frac{h}{2} < z < z_o + md_o + \frac{h}{2} \\ &= 0 \quad \text{otherwise} \end{aligned} \tag{5.A.14}$$

where m is a positive or negative integer or zero, and z_o is the center of one of the absorbers. Hence, instead of the result S from our system, we will have the result, for any $U(z)$,

$$S_G = \int_{z_{\min}}^{z_{\max}} D(z)U(z)G(z)dz, \tag{5.A.15}$$

Because $G(z)$ is periodic, we can expand it in a cosine series about the point z_o. If we presume that h is always small compared to any wavelength of interest, then the result is particularly simple, and we obtain

$$G(z) \cong \frac{2h}{d_o}\left[\frac{1}{2} + \sum_{p=1}^{\infty} \cos(pk_o(z - z_o))\right] \tag{5.A.16}$$

where

$$k_o = \frac{2\pi}{d_o}. \tag{5.A.17}$$

Formally evaluating S_G from (5.A.15) gives

$$S_G = \frac{2h}{d_o}\left[\frac{S}{2} + \sum_{p=1}^{\infty} \int_{z_{\min}}^{z_{\max}} D(z)U(z)\cos(k_o(z - z_o))dz\right]. \tag{5.A.18}$$

Now again let us suppose that $U(z)$ is a cosine wave as given by (5.A.9). To get our desired result, we need to choose the position of the "comb" of absorbers such that one of the "comb" is centered at the point $z = 0$. This point will correspond, for example, to the position of the mirror in the case of a standing wave formed by reflection off a mirror with no phase change on reflection. This allows us to choose $z_o = 0$ without loss of generality. The physical meaning of this choice of the positioning of the "comb" is that, at a wavevector k_o, all of the absorbers lie at antinodes of such a wave. (Note that there need not be an actual absorber at $z_o = 0$, since the integration limits might not include this point, but the mathematical "extension" of the comb should have an element at $z_o = 0$.)

If we presume that the integration limits are effectively infinite, after some algebra, we can write the result

$$S_G \propto \sum_{p=0}^{\infty} \left\{ I_{\text{inc}}\left(\left[k' + p\frac{k_o}{2}\right]\frac{c}{n}\right) + I_{\text{inc}}\left(\left[k' - p\frac{k_o}{2}\right]\frac{c}{n}\right)\right\}. \tag{5.A.19}$$

(Note that, formally, the range of p now starts at zero.) The meaning of (5.A.19) is that the system now not only detects the incident intensity at frequency $\omega = k'c/n$, but also at all the positive "sideband" frequencies spaced at integer multiples of a sideband-spacing frequency

$$\Delta\omega = \frac{\pi c}{n d_o}. \tag{5.A.20}$$

This detection of sideband frequencies could be undesirable if the range of input frequencies is such that two of them could be simultaneously detected with the same $U(z)$. At the very most, we can uniquely discriminate frequencies within a range just less than $2\Delta\omega$.

One useful feature of these sidebands is that we can detect a particular frequency, ω_d, of wave without having to space the detectors more closely than the wavelength. We can have much more widely spaced detectors, and use them to detect a high sideband frequency. In fact we could choose any $d_o = p\pi c/n(\omega_d - \omega)$. Of course, spacing the detectors progressively further apart does make them sensitive to other wavelengths progressively closer to the wavelength of interest (i.e., reducing the "free spectral range").

If we have finite integration limits in (5.A.18), then instead of sharp response at the exact frequencies as in (5.A.19) we will have the "$\sin(f)/f$" resolution function response, as described in (5.A.11) and (5.A.13), round about each of the exact frequencies.

For the simple example detector structure of Fig. 1, the detectors are alternately weighted by $+1$ and -1; this corresponds to a sampling wavevector $k' = \pi/2d_o$. Based on

the above model (or, equivalently, a straightforward first-principles model for this simple case), we can deduce that this detector system gives equal outputs at wavelengths

$$\lambda_m = \frac{4nd_o}{2m+1} \tag{5.A.21}$$

where m is a positive integer or zero.

For a detector system with an equally spaced set of detectors, starting with one on the mirror, and assuming no phase change on reflection off of the mirror, the resolution of the detector in wavelength will be, from (5.A.13),

$$\delta\lambda = \frac{\lambda^2}{2nz_{\max}} \tag{5.A.22}$$

where this $\delta\lambda$ corresponds to the full width to the first zero on either side of the main peak.

Although it is simplest to make detector systems with weights of only $+1$ and -1, it is possible to have other weights. We can change the weights either in the fabrication, or by controlling the amount of absorption by some other means, such as electric field. To change the weights by fabrication in a longitudinal detector, we can change the relative absorption of those layers by making specific absorbing layers thicker or thinner. If the layers are quantum wells, the absorption may not change proportionately with thickness; in this case, we could achieve other low integer weights by puting more than one quantum well close together at the appropriate points so that they are all approximately sampling the same point in the standing wave. The weight would increase approximately proportionally with the number of such wells. For a transverse detector, we could change the weights by choosing different widths for the detecting elements. In either the longitudinal or transverse cases, we could also change the weights after fabrication if we could change the amount of absorption by changing the voltage on the individual detecting elements. For semiconductor systems, the absorption could be changed through the Franz-Keldysh effect for bulk semiconductor layers, and through the quantum-confined Stark effect for quantum wells, for example.

All the modeling in this section so far has used the notation for a longitudinal grating at normal incidence to the mirror. The analysis also applies to the transverse case if we substitute $n\sin\theta$ for n and x for z throughout this section (where θ is the angle of incidence relative to the normal to the detector plane in the transverse grating case—see Figs. 6 and 7).

We can illustrate the simple cases of $+1$ and -1 weights with specific example designs. For a longitudinal detector, for example, for sensitivity at a free-space wavelength of 850 nm, in a material with refractive index $n = 3.5$, and $m = 16$ (i.e., 8.25 wavelengths in the material between detecting elements (see 5.A.21)), the spacing d_o between adjacent detectors will be approximately 2.004 μm, and the detector will give an equally large signal at the adjacent wavelengths of 801 nm and 905 nm (on the assumption that the absorbers absorb equally at these other wavelengths). For a total of 16 detectors, corresponding to $z_{\max} = 32.06$ μm, the "width", $\delta\lambda$, of the sensitivity peak would be about 5 nm. We can also give an example design for a 16 detector transverse structure, also with

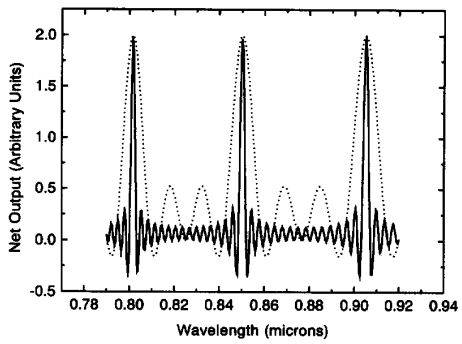

Fig. 9. Net output from a 4-element (dotted line) and a 16-element (solidline) detector system designed for high sensitivity at 850 nm. The elements are equally spaced, and are weighted alternately $+1$ and -1 in summing for the net output. The spacing between detector elements corresponds to 8.25 wavelengths at 850 nm.

$m = 16$, which will have the same wavelength performance as this longitudinal structure. With waves incident from free space (so that $n = 1$), at an angle of $\theta = 5°$, we would have a spacing between adjacent detectors of 80.5 μm for a peak sensitivity at 850 nm. Such a detector would also be sensitive at 801 nm and 905 nm. The solid line in Fig. 9 shows the resulting performance for these two detectors. The dotted line in Fig. 9 shows the results for a similar structure, but with 4 detectors rather than 16. Note that in both of these designs, the first detector is positioned at the mirror surface (or at the intersection of the mirrors in the transverse case), and we have assumed no phase change on reflection off of the mirror.

In general, we can implement this class of wavelength sensitive detector with a structure of the form of the structure in Fig. 1, with independent connections to each detector. In practice, this may be difficult to achieve because the layers in such a longitudinal structure may be close together, although this could be achieved using existing techniques with some effort (e.g., through multiple layers of lithographic patterning, etching, and contacting). The use of a transverse structure, however, might allow large numbers of detectors to be used because it would not necessitate the growth of a thick structure, and it might be easier to make the separate connections to all of the detector elements. Using a single "layer" of conventional photolithographic processing, it is possible to make separate contacts to each detecting element, and hence to feed them separately, with appropriate electronic weights, for summing. If those weights are controlled electrically, this detector could be fully tunable.

Fig. 10 shows a transverse detector with $+1$ and -1 weights for narrow band detection, illustrated here for the case of 8 detector elements. In this case, rather than patterning the absorber directly, we pattern the conductivity of a p-layer in a p-i-n diode. In use, the diodes will be reverse biased. Everywhere that the p-layer has not been implanted, there will be a field applied across the diodes, and any photocurrent will be swept out. It might also be useful to extend the implantation into the quantum well region to suppress any undesired photocurrent that might otherwise be collected from

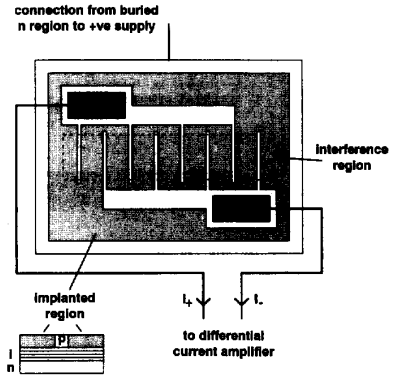

Fig. 10. Schematic diagram of transverse-grating, narrow-band detector. In the grey regions, the top p-layer of the diode is implanted, for example with protons, to make it insulating. The figure shows a top view, and also a side view of one detector element to illustrate the implanted regions.

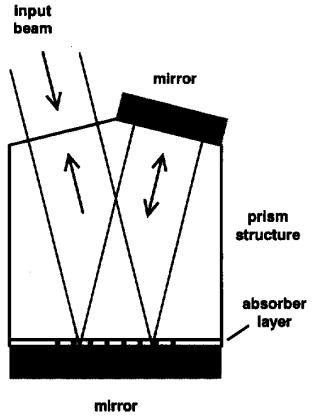

Fig. 11. Example structure for the use of a transverse absorption grating device.

these regions. This system has the advantage of being fully self-aligned; there is no need to align the patterning of the absorber and the conducting contact layers over the absorbers. Where there is no implant, a conducting p-layer is left, needing no other deposited conducting material. Such a self-aligned process allows particularly narrow conducting p-regions to be made. With this structure, there are no mesa etches or metallic contacts within the interference region, so the grating structure is not apparent to the light beam to give diffraction in any other way. This device could conveniently be used in the mode where reverse bias on the diode turns on the absorption, as could be achieved with quantum wells. When used in this way, there would be no absorption in the regions underneath the implanted regions, without having to pattern the absorber material itself. Note in this case that different weights (of a given sign) could be set by fabricating different widths of detector.

Fig. 11 shows an example of a structure that could be used with transverse absorption gratings, either as a wavelength sensitive detector discussed here, or as a laser tuner, especially for linear laser cavities. The solid prism structure holds the mirrors and the absorber layer at fixed distances. In use, the entrance surface of the prism structure could be anti-reflection coated, especially for laser tuner applications. The entrance face could also be deliberately slightly misaligned so that the small reflection from this face was not an exact retroreflection; this misalignment would avoid undesired etalon effects between this surface and the top mirror; a similar misalignment between the front and back faces is common in laser output couplers for the same reason.

Because the beams in Fig. 11 are travelling essentially perpendicular to the prism surface on entrance and exit, the prism is essentially nondispersive, allowing the wavelength sensitivity to be controlled by the absorbers. Although shown in Fig. 11 for the case of exactly counterpropagating beams, this is not necessary for detector applications; in fact, avoidance of exact counterpropagation could be desirable to prevent feedback. Of course, when used as a tuner in a linear laser cavity, the beams will be exactly counterpropagating.

B. Other Device Structures

Single-Absorber Longitudinal Standing Wave Detector: One of the simplest wavelength sensitive detector structures is a single absorber in a standing wave. Fig. 12 illustrates the structure. This detector gives a large output when the antinode of the standing wave coincides with the absorber at distance d from the mirror, and close to zero output when a node coincides with the absorber. The solid curve in Fig. 13 shows the response of this detector for a specific design. The response is approximately sinusoidal with wavelength. Normally when we use a semiconductor to make a detector, it is straightforward to have the detector respond to short wavelengths but not to long wavelengths; the cut-off wavelength between the two regions is simply the optical absorption edge of the semiconductor. Many applications, however, require the opposite property of responding to a longer wavelength but not to a shorter one. An example would be detectors for a two-color wavelength division multiplexed communications system. Detectors for the shorter wavelength that did not detect the longer wavelength could simply be made with an appropriate choice of semiconductor bandgap, but to detect the longer wavelength without detecting (or even absorbing) the shorter one is more difficult; this detector structure can clearly perform the required function by choosing the shorter wavelength to correspond to a minimum in the detector response.

Two-Absorber Longitudinal Standing Wave Detector: A structure with two absorbing layers in separate detector circuits has several possible functions. Fig. 14 shows the structure schematically.

One way of constructing such a two-absorber detector is shown in Fig. 15. Here the two detectors are made as p-i-n photodiodes. The two diodes share a common p-layer for simplicity in the structure. The necessary signals could be extracted as the currents from the two n-layer contacts, with the p-layer contact serving as a common ground connection.

Simple Narrow Band Detector For a simple narrow band detector, d_b is chosen to be $2d_a$, and we subtract the outputs from the two detectors. This effectively cancels every second

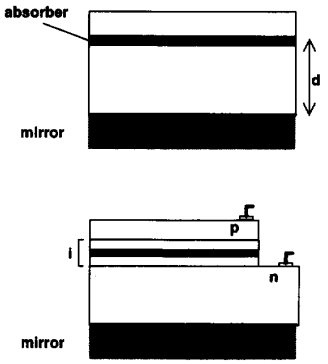

Fig. 12. single-absorber wavelength-sensitive detector. (a) Generic form, with the absorber (black region) centered a distance d away from the mirror. (b) Specific implementation, with the absorber contained within a p-i-n diode. For a reverse biased diode, the detected signal could then be the current from the diode.

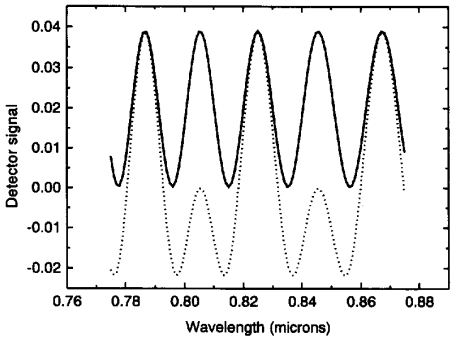

Fig. 13. Output signal (for unit input amplitude) for a single-absorber detector (solid line) and a particular two-absorber detector (dotted line). The single-absorber detector has one 10 nm thick absorber centered at a distance 5.775 μm from a 100% reflecting mirror with no phase change on reflection. For the two-absorber case, a second absorber is added centered round half this distance (i.e., at 2.888 μm); the detector signal in this case is the difference between the signals from the first and second absorbers. All layers have refractive index 3.5. The absorbers have an absorption coefficient of 10^4 cm^{-1}. The distances correspond to 24.5 and 12.25 wavelengths from the mirror respectively for the first and second absorbers at a wavelength of 825 nm. These calculations use the exact method. The input is presumed to be of unit intensity, and the signal units correspond to one unit of signal for total absorption of the incident wave in a single absorber.

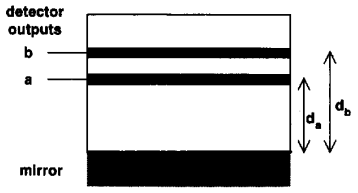

Fig. 14. Two detectors, a and b, with absorbing layers shown as the black regions, are positioned in the standing wave pattern at fixed distances relative to the mirror. The structure is assumed to be antireflection coated (not shown) on the top surface in this example.

maximum of the single-absorber detector discussed above. When there is an antinode at detector a, we may have a node at detector b; this will give exactly the same signal as the single-absorber detector discussed above; however, at the next

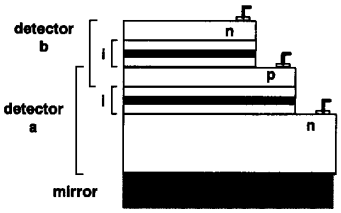

Fig. 15. Example structure for the two-absorber detector of Fig. 14. The black layers are the absorbing regions for the detectors. The other layers are transparent at the wavelengths of interest.

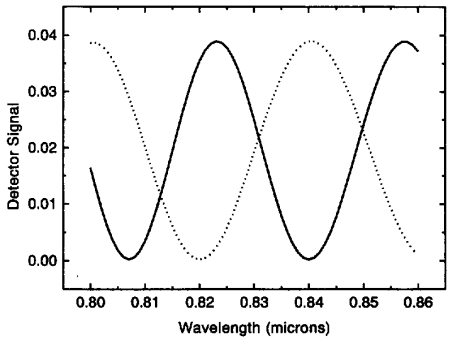

Fig. 16. Detected signals from detector a (dotted line) and detector b (solid line) in a two-wavelength detector. Absorber a is centered at a distance 2.401 μm from a 100% reflecting mirror with no phase change on reflection. Absorber b is centered at a distance 2.940 μm from the same mirror. Both absorbers are 10 nm thick and have an absorption coefficient of 10^4 cm^{-1}. All layers have refractive index 3.5. Detector a gives a strong signal at 840 nm and essentially no signal at 820 nm; detector b gives a strong signal at 820 nm and essentially no signal at 840 nm. The distances correspond to detector a being 10.25 wavelengths at 820 nm from the mirror and detector b being 12.25 wavelengths at 840 nm from the mirror.

wavelength at which we have an antinode at detector a, we will also have an antinode at detector b, and so the net signal after subtraction will be zero. The actual response of such a detector is shown as the dotted line in Fig. 13. Note also that this detector has true zeros in its wavelength response, since the response goes from positive to negative.

two-Wavelength Detector: For a two-wavelength detector, detector a is chosen to be near an antinode for the first wavelength and at a node for the second, hence detecting signals at the first and not the second wavelength; detector b has the situations reversed so that it detects the second wavelength and not the first. (Note that it is not possible mathematically to have both detectors exactly at antinodes for their desired wavelengths while simultaneously being exactly at nodes for the other wavelengths.) Fig. 16 shows the response from the two detector elements for a structure designed to detect 820 nm and 840 nm signals separately.

A detector such as this could also give a useful estimate of the wavelength derivative of a continuous spectrum within, for example, the spectral region 820–840 nm. It would of course be necessary to filter out other spectral ranges to avoid confusion.

Wavelength-Measuring Detector When the input to the detector of Fig. 14 is predominantly monochromatic, we can

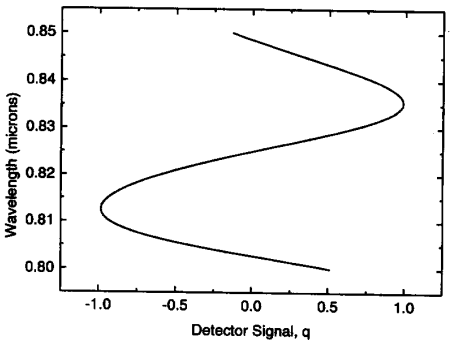

Fig. 17. Relation between the wavelength of a beam and the detector signal for the wavelength-measuring detector of Fig. 14. The calculated structure has distances $d_a = 1.915$ μm and $d_b = 2.328$ μm (measured to the center of the absorbing layers), with a refractive index of 3.5 throughout. The solid line is a calculation using the exact theory, with 10 nm thick absorbers of 10^4 cm^{-1} absorption coefficient. A calculation using the simple approximate theory, assuming the absorbing layers are thin compared to a wavelength, gives almost identical results, within the width of the plotted line. At a wavelength $\lambda = 825$ nm, the separation between the centers of the absorbing layers, $d_a - d_b$ corresponds to $7\lambda/4$, and the distance from the mirror to the center point between the layers, $(d_a + d_b)/2$, corresponds to 9λ.

deduce the wavelength of the incident radiation from the relative responses of detectors at different points in the standing wave pattern.

There are several ways in which we could process the signals from the two detectors to deduce the wavelength. For example, if the absolute power in the incident beam is known, we can deduce the wavelength from the difference in signals. Alternatively, to avoid having to measure the power separately, we could use the ratio of the two signals. The ratio may be inconvenient since it can vary very greatly, and can even become singular when one of the signals is zero. A third possibility is to use the quotient

$$q = \frac{a-b}{a+b} \tag{5.2.1}$$

where a and b represent the signals from the two detectors respectively, which also avoids a separate power measurement.

We can analyze this device using the simple theory of section 4.A.1. For the simple case of a 100% reflecting mirror with no phase change on reflection, q is, from (4.A.1),

$$q = \frac{\cos 2kd_a - \cos 2kd_b}{2 + \cos 2kd_a + \cos 2kd_b} = \frac{\sin(k(d_a + d_b))\sin(k(d_a - d_b))}{1 + \cos(k(d_a + d_b))\cos(k(d_a - d_b))}. \tag{5.2.2}$$

This expression is not readily invertible analytically to give k (and hence the wavelength $\lambda = 2\pi/k$), and does not, of course, give a unique value for the wavelength. There are many different wavelengths that can give the same ratio, depending on how many half wavelengths fit into the region between the detectors and the mirror. Within a given range of wavelengths, however, a unique answer is possible. Fig. 17 gives an illustrative calculation showing the relation between q and λ for a particular layer structure.

As can be seen from the representative calculation in Fig. 17, for a particular range of wavelengths (e.g., 815 nm to 835 nm) there is a smooth relation between the measurement q and the incident wavelength. This relation is relatively linear between 820 nm and 830 nm for this example. This calculation also shows that, at least for this structure, the simple theory of Section 4.A.1 does give a reasonable approximation to the behavior of the structure. We will use the simple theory to derive some analytic results that will help in the design of such structures.

Based on the simple theory, we can find an expression for the sensitivity of this wavelength measuring detector. We will evaluate this for the case of $q = 0$, which corresponds to the center of the wavelength sensitive regions.

From (5.2.2), there are clearly two ways of achieving $q = 0$, either (i) $\sin(k(d_a + d_b)) = 0$, or (ii) $\sin(k(d_a - d_b)) = 0$. We can trivially rewrite

$$\sin(k(d_a + d_b)) \equiv \sin\left(2k\frac{(d_a + d_b)}{2}\right),$$

which allows us to see that case (i) corresponds to either a standing wave node or a standing wave antinode centered between the two absorbing layers. (The sine equal to zero implies the cosine is + or −1. From (4.A.1), a cosine of +1 corresponds to an antinode, and a cosine of −1 corresponds to a node.) Case (ii) can be seen to correspond to the case where there is an integer number of half wavelengths separating the two absorbing layers.

Case (i) is the more interesting one practically because $\sin(k(d_a + d_b))$ changes faster with wavelength than does $\sin(k(d_a - d_b))$, resulting in greater sensitivity for case (i). After some algebra, we obtain for this case ($\sin(k(d_a + d_b)) = 0$)

$$\left.\frac{dq}{dk}\right|_{\sin(k(d_a+d_b))=0} = \pm(d_a + d_b)\frac{\sin(k(d_a - d_b))}{1 \pm \cos(k(d_a - d_b))}, \tag{5.2.3}$$

or, equivalently,

$$\left.\frac{dq}{d\lambda}\right|_{\sin(k(d_a+d_b))=0} = \mp\frac{2\pi}{\lambda^2}(d_a + d_b)\frac{\sin(k(d_a - d_b))}{1 \pm \cos(k(d_a - d_b))}, \tag{5.2.4}$$

where the upper sign refers to the case of an antinode centered between the absorbing layers, and the lower sign refers to a node.

Given that we will be operating the device round about points for which $\sin(k(d_a + d_b)) = 0$, we can deduce the separation, in wavelength or wavevector, between such points. + or − half of this number will also give approximately the maximum usable wavelength or wavevector range around a such an operating point. Hence we obtain, for the usable wavevector range

$$\Delta k \approx \pm\frac{\pi}{2(d_a + d_b)}, \tag{5.2.5}$$

about an operating point wavevector

$$k_p = p\frac{\pi}{(d_a + d_b)}, \tag{5.2.6}$$

where p is an integer expressing the number of half wavelengths between the mirror and the center point between the

two absorbers. Equivalently, the usable wavelength range is approximately

$$\Delta\lambda \approx \mp \frac{\lambda_p^2}{4n(d_a + d_b)}, \tag{5.2.7}$$

where n is the refractive index and we are expressing in terms of free-space wavelengths, and the operating point wavelength is

$$\lambda_p = \frac{2n(d_a + d_b)}{p}. \tag{5.2.8}$$

For the example structure of Fig. 17, p is 9, corresponding to 9 half-wavelengths, and $\Delta\lambda \approx \pm 11.5$ nm.

We can see from (5.2.3) and (5.2.4) that we should avoid setting the separation between the absorbers at an integer number of half waves since we may obtain zero sensitivity (the numerator will be zero). Furthermore, it is also clearly possible to have the denominator also equal to zero; this can occur either for an antinode centered between the absorbing layers and $\cos(k(d_a - d_b)) = -1$, or a node centered between the layers and $\cos(k(d_a - d_b)) = +1$. Both of these troublesome situations with the numerator equal to zero correspond to situations where we have nodes at both absorbers, and hence zero power detected, clearly an undesirable situation physically.

One design that avoids the problems of zero numerators and denominators is to choose the separation between the absorbing layers to be an odd number of quarter wavelengths. In this case $\sin(k(d_a - d_b)) = \pm 1$ and $\cos(k(d_a - d_b)) = 0$, and the magnitude of the sensitivity becomes

$$\left| \left. \frac{dq}{dk} \right|_{\substack{\sin(k(d_a+d_b))=0 \\ \sin(k(d_a-d_b))=\pm 1}} \right| = d_a + d_b \tag{5.2.9}$$

or, equivalently,

$$\left| \left. \frac{dq}{d\lambda} \right|_{\substack{\sin(k(d_a+d_b))=0 \\ \sin(k(d_a-d_b))=\pm 1}} \right| = \frac{2\pi n}{\lambda^2}(d_a + d_b). \tag{5.2.10}$$

The structure in Fig. 17 corresponds to this situation. (5.2.10) gives

$$\left| \left. \frac{dq}{d\lambda} \right|_{\lambda=825 \text{ nm}} \right| = 0.137 \text{ nm}^{-1}$$

for the structure in Fig. 17 at 825 nm.

VI. Laser Tuning

There are many different device structures that can be used for laser tuning. One general point is that the absorbers in multiple absorber tuners (as in Fig. 2) need not be spaced every half wavelength, but can be spaced several half wavelengths apart. Just as with detectors, as discussed above in Section 5.A, there will be multiple wavelengths at which there is minimum absorption. If the bandwidth of the laser is restricted by some other means so that only one of these minima lies within the overall bandwidth of the laser, then we will still get a unique laser output wavelength. This gets round the limitation that some ideas would be difficult to make otherwise because the absorber layers would have to be spaced too closely.

A. Tuner with Selectable Wavelength

One simple concept for making a laser with a selectable wavelength is to make several absorbing sections, each one containing a grating of absorbers as in Fig. 2. If the absorption of each of these sections can be controlled by voltage, as could be the case for semiconductor absorbers, we could arrange to "turn on" the set of absorbers in one section and "turn off" the absorbers in the other sections. Then the wavelength would be set by the spacing of the absorbers in the section that was "turned on". By this means, we could choose which of several pre-determined wavelengths would lase. Such a structure could be made with several stacked p-i-n diodes, each containing one or more absorbers within its intrinsic (i) region. It could also be made with a transverse grating structure with several different absorbing gratings, each of which could be separately turned on or off.

B. Continuous Tuning of a Laser Using Controllable Absorbing Layers

Various schemes could be derived to make a laser oscillate at particular wavelengths by turning on and off specific absorbing layers in extensions of the scheme discussed above. Another variation is to make a device that allows continuous tuning of the laser. In this case, we make a structure in which the absorption in one or more layers can be continuously varied. As we vary this absorption, the wavelength of minimum absorption can be continuously varied. Because the laser will tend to run at wavelengths that minimize its absorption, we can use this method to tune the laser continuously over some range of wavelengths.

To be strictly correct, the laser will always have to run in a cavity mode, which means that it can only run in one of a discrete set of wavelengths, with each wavelength in the set corresponding to one of the cavity modes. This method allows us to choose the mode in which the laser oscillates. In this sense, this method is different from refractive laser tuning methods that actually change the optical length of the cavity; such a refractive method gives a truly continuous tuning of the laser wavelength, although hopping to other cavity modes is possible if such a method attempts to tune by more than one cavity mode separation. In practice, with this absorptive method, by making the cavity length sufficiently long, we can make the cavity modes as close together as we wish, and hence we can achieve tuning with steps as small as we wish.

We can make such an absorptive, "continuous" tuner using structures similar to those shown in Figs. 14 and 15. In the present case, the absorbing layers are used as controllable absorbers rather than detectors. If the layers are quantum wells, the absorption can be controlled by changing the bias voltages on the two p-i-n diodes in the structure of Fig. 15. Changing the bias voltage changes the absorption of a given layer through the quantum-confined Stark effect in wavelength regions close to the optical absorption edge. It may also be possible to use other electroabsorptive mechanisms, such as the Franz-Keldysh effect, in semiconductor structures not exhibiting the quantum-confined Stark effect.

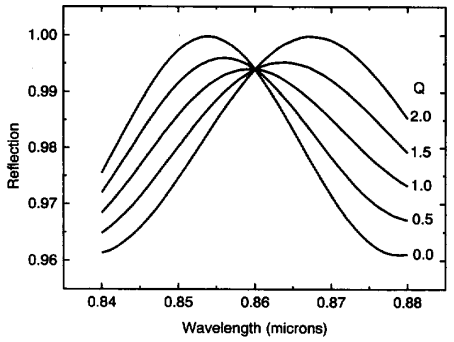

Fig. 18. Reflection calculated as a function of wavelength for a two layer absorber for various relative absorptions in the two layers. The parameter Qindexes the relative absorption in the layers. $Q = 0$ corresponds to no absorption in layer a, and full absorption in layer b, and $Q = 2$ corresponds to the opposite condition (a absorbing and b not). The absorption varies linearly with Q between these extremes. As Q is varied from 0 to 2, the wavelength of maximum reflection varies from approximately 854 nm to approximately 867 nm, which indicates the likely tuning range. The peak reflection remains high (> 99.3%) for all values of Q shown. The specific structure here has 10 nm thick absorbing layers with peak absorption coefficient of 10^4 cm^{-1}. The distances from the mirror to the centers of the layers are $d_a = 1.797$ μm and $d_b = 2.135$ μm, and the refractive index is assumed to be 3.5 throughout. These thicknesses correspond, at a (free-space) wavelength of 860 nm, to a distance of 8 wavelengths from the mirror to the center point between the two absorbing layers, and a separation of the centers of the absorbing layers of 11/8 wavelengths.

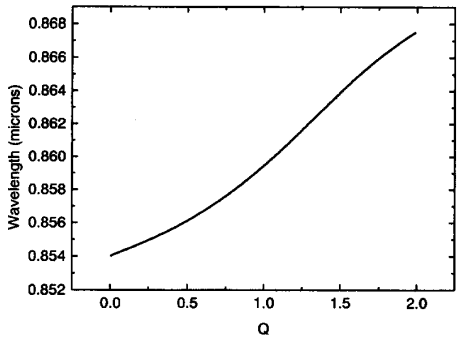

Fig. 19. Wavelength tuning curve for the structure used for Fig. 18. Q is the parameter that varies the relative absorption in the two absorbing layers.

Fig. 18 shows reflection as a function of wavelength for a particular design for several different values of the relative absorption in the layers. For the purposes of this figure, the absorption in the two layers is presumed to vary linearly with some parameter Q between zero and a peak value, i.e.,

$$A_a = A_{1/2}Q \tag{6.B.1}$$

and

$$A_b = A_{1/2}(2 - Q) \tag{6.B.2}$$

where A_a and A_b are the (single-pass) absorptions of layers a and b respectively, and $A_{1/2}$ is half of the peak absorption of a given layer. With this choice, Q runs from 0 to 2.

A design such as this could be implemented with GaAs quantum wells as the controllable absorbers in a diode structure such as that of Fig. 15. This particular design offers a tuning range of about 13 nm. The absorption of a GaAs quantum well could be controlled over this wavelength region through the quantum-confined Stark effect.

A calculation using the simple approximate theory yields results almost indistinguishable from those of Fig. 18. The only noticeable difference is a slightly greater absorption (0.1%) at the minimum reflection points, which is easily understood because the simple theory neglects the absorption in calculating the standing wave pattern and hence overestimates the strength of the standing wave pattern maxima in the presence of absorption. Incidentally, the fact that all of the curves pass through the same reflection at 860 nm (an isosbestic point) in Fig. 18 is a simple artifact of the assumption that the absorption in the two absorbers varies linearly with a constant total ((6.B.1) and (6.B.2) above). At 860 nm, by design, the standing wave amplitude is equal at both absorbers, hence the total absorption is the same for all Q.

We can use the simple theory to derive some simple analytic results since it appears to work reasonably well when compared with the exact model. One useful result is the tuning curve. In the simple model, the total absorption in the structure is

$$A_{\text{tot}} = 2[A_a(1 + \cos 2kd_a) + A_b(1 + \cos 2kd_b)]. \tag{6.B.3}$$

The wavevectors (or wavelengths) of minimum (or maximum) absorption are found by differentiation. Hence we have to solve the equation

$$d_a A_a \sin 2kd_a + d_b A_b \sin 2kd_b = 0, \tag{6.B.4}$$

which can be done numerically. Fig. 19 shows the result for the example structure used for Fig. 18, which shows the tuning curve (strictly, the wavelength of minimum loss as a function of Q).

We could also envisage stacked versions of such tuners, with different spacings relative to the mirror, to make more selective structures. This could use principles similar to those used for multiple plate Lyot tuners.

C. Tuners with Transverse Gratings

All of the ideas presented for longitudinal laser tuner structures could be implemented in transverse structures. Just as for detectors, as discussed in Section 5.A, we should substitute $n \sin \theta$ for n and x for z where θ is the angle of incidence relative to the normal to the detector plane in the transverse grating case (see Figs. 6 and 7). In the transverse case, n is the refractive index in the medium in which the wave is incident, not in the absorbing region.

The transverse structures would be particularly well suited for tuners that needed a large number of absorbers, such as tuners with narrow bandwidths or tuners with many preset tuning sections to be turned on and off. In general, it is easier to make devices requiring many separate connections to layers or sets of layers in the transverse configuration because only a single lithographic step is required to define these many separate connections. We could use a fabrication method similar to that used for the detector structure of Fig. 10. For the

case of the laser tuner, it would be particularly useful to control the absorptions of individual absorbers, turning them on and off (or changing their value) with applied voltage. Within the interference region, the conducting regions could be defined by implantation as in Fig. 10, although in the laser tuner case we might make individual connections to the conducting regions rather than the specific scheme shown in Fig. 10.

D. Laser Phase Controller

The laser tuner structures, when used in a bidirectional ring laser cavity, will also control the relative phase of the forward and backward propagating waves. Their relative phase will tend to line up so as to minimize the absorption in the absorbing structure. For example, a thin absorber at a particular position will tend to cause the forward and backward waves to interfere destructively at this point. As another example, we could use the continuous laser tuner structure of Section 6.B for a continuous variation of the relative phase. Adjusting the relative absorption in the two absorbers would adjust the node position of minimum loss, hence adjusting the relative phase of forward and backward waves in the laser because of the laser's tendency to run under the condition of minimum loss.

VII. Conclusion

We have proposed a new method for making laser tuners and wavelength-sensitive or tunable detectors that is based on absorbers in a standing wave. This method allows a large variety of novel devices. It is particularly well suited to modern semiconductor fabrication techniques, and may allow integrated wavelength-sensitive and tunable systems.

One form of these devices uses a longitudinal standing wave pattern, which can be formed by a simple back reflection; devices of this longitudinal form could be made using multiple layered semiconductor structures. The other form uses a transverse standing wave pattern, which can be formed by interfering beams at an angle on a surface; this transverse form is suited to lithographically patterned structures.

We have presented theoretical models for these structures, which allow design of a variety of devices. These models include a simple theory for both device forms, and a complete model for the longitudinal form that includes all the effects of finite absorption. We have also discussed a general method for detecting any frequency of wave with a fixed, multiple-absorber structure; this method enables tunable detectors whose sensitivity can be controlled entirely electrically, either through electrical control of the mathematical weights in summing the detector signals, or through physical control of the amount of absorption in the detectors by electroabsorption.

We have also illustrated the concepts with various specific device structures. These include (a) a narrow band detector based on transverse gratings, (b) a simple wavelength sensitive longitudinal structure with a single absorber, and (c) a two-absorber longitudinal structure capable of many functions, including a narrow band detector, a two-wavelength detector, a wavelength measuring detector, a continuously variable laser tuner, and a laser phase controller.

Unlike many other methods of making such detectors or tuners, this method does not rely on mechanical changes in position or on changes in refractive index. Consequently it may offer high-speed tunable devices whose range is not constrained by limits on the size of refractive index changes. The tuning range of the laser tuners and some of the detectors is limited by the spectral range over which the absorption can be changed. For detectors tuned by varying electrical weights in a summation, the tuning range is limited only by the form of the absorption spectrum itself.

Quantum wells are particularly useful for the absorbers in longitudinal devices because they are conveniently much thinner than a wavelength, and hence effectively sample the standing wave pattern at a specific point. Quantum wells also allow the absorption strength to be changed with voltage as desired for the tunable devices. Useful devices could also be made with bulk semiconductor structures, especially in transverse structures.

The fact that the devices could be made by layered semiconductor growth and lithographic patterning techniques means that the resulting devices may be small, light and readily manufacturable. These devices may find applications in wavelength-division multiplexing and switching in communications networks, sensors, and spectroscopy, where their convenient operation, small size, and manufacturability may open up new practical applications.

Acknowledgment

I am pleased to acknowledge stimulating conversations with Luca Carraresi.

References

[1] U. Prank, M. Mikulla and W. Kowalsky, "Metal-semiconductor-metal photodetector with integrated Fabry–Perot resonator for wavelength demultiplexing high bandwidth receivers," *Appl. Phys. Lett.* **62**, pp. 129–130 (1993).

[2] M. Jestl, A. Köck, W. Beinstingl and E. Gornik, "Polarization-and wavelength-selective photodetectors," *J. Opt. Soc.* Am. A, **5**, pp. 1581–1584 (1988).

[3] G. Strasser, K. Bochter, M. Witzany and E. Gornik, "Improved tunable InSb FIR detectors," Infrared Physics **32**, pp. 439–442 (1991).

[4] A. Köck, E. Gornik, G. Abstreiter, G. Böhm, M. Walther and G. Weimann, "Double wavelength selective GaAs/AlGaAs infrared detector device," *Appl. Phys. Lett.* **60**, pp. 2011– 2013 (1992).

[5] E. Martinet, F. Luc, E. Rosencher, Ph. Bois and S. Delaitre, "Electrical tunability of infrared detectors using compositionally asymmetric GaAs/AlGaAs multiquantum wells," *Appl. Phys. Lett.* **60**, pp. 895–897 (1992).

[6] B. F. Levine, C. G. Bethea, V. O. Shen and R. J. Malik, "Tunable long-wavelength detectors using graded barrier quantum wells grown by electron beam source molecular beam epitaxy," *Appl. Phys. Lett.* **57**, pp. 383–385 (1990).

[7] T. H. Wood, C. A. Burrus, A. H. Gnauck, J. M. Wiesenfeld, D. A. B. Miller, D. S. Chemla and T. C. Damen, "Wavelength selective voltage-tunable photodetector made from multiple quantum wells," *Appl. Phys. Lett.* **47**, pp. 190–192 (1985).

[8] A. Larsson, P. A. Andrekson, S. T. Eng and A. Yariv, "Tunable superlattice *p-i-n* photodetectors: Characteristics, theory, and applications," *IEEE J. Quantum Electron.* **24**, pp. 787–801 (1988).

[9] S. Goswami, P. Bhattacharya and J. Singh, "Wavelength selective detection using excitonic resonances in multiquantum-well structures," *IEEE J. Quantum Electron.* **27**, pp. 875–877 (1991).

[10] T. L. Koch and U. Koren, "Semiconductor lasers for coherent optical fiber communications," *J. Lightwave Technol.*, **LT-8**, pp. 274–293 (1990).

[11] R. C. Alferness, U. Koren, L. L. Buhl, B. I. Miller, M. G. Young, T. L. Koch, G. Raybon and C. A. Burrus, "Broadly tunable InGaAsP/InP laser based on a vertical coupler filter with 57 nm tuning range," *Appl. Phys. Lett.* **60**, pp. 3209–3211 (1992).
[12] M. Kuznetsov, P. Verlangieri, A. G. Dentai, C. H. Joyner and C. A. Burrus, "Asymmetric Y-branch tunable semiconductor laser with 1.0 THz tuning range," *IEEE Photon Tech. Lett.* **4**, pp. 1093–1095 (1992).
[13] M. Schilling, K. Dütting, W. Idler, D. Baums, G. Laube, K. Wünstel and O. Hildebrand, "Asymmetrical Y-laser with simple single current tuning response," *Electron. Lett.* **28**, pp. 1698– 1699 (1992).
[14] V. Jayaraman, D. A. Cohen and L. A. Coldren, "Demonstration of broadband tunability in a semiconductor laser using sampled gratings," *Appl. Phys. Lett.* **60**, pp. 2321–2323 (1992).
[15] B. Glance, U. Koren, R. W. Wilson, D. Chen and A. Jourdan, "Fast optical packet switching based on WDM," *IEEE Photon. Tech. Lett.* **4**, pp. 1186–1188 (1992).
[16] Y. V. Troitskii, "Optical resonator with a thin absorbing film as a mode selector," *Optics and Spectroscopy*, **25**, pp. 309–313 (1968).
[17] W. R. Leeb, "Tunable metal film filters as narrowband ir laser reflectors," *Applied Optics*, **15**, pp. 681–689 (1976).
[18] A. M. Glass, P. F. Liao, D. H. Olson and L. M. Humphrey, "Optical metal-oxide tunnel detectors with microstructured electrodes," *Optics Lett.*, **7**, pp. 575–577 (1982).
[19] A. M. Glass, P. F. Liao, A. M. Johnson, L. M. Humphrey, R. Lemons, D. H. Olson and M. B. Stern, "Periodically structured amorphous silicon detectors with improved picosecond responsivity," *Appl. Phys. Lett.* **44**, pp. 77–79 (1984).
[20] D. A. B. Miller, D. S. Chemla, T. C. Damen, A. C. Gossard, W. Wiegmann, T. H. Wood and C. A. Burrus, "Electric field dependence of optical absorption near the band gap of quantum-well structures," *Phys. Rev.* B, **32**, pp. 1043–1060 (1985).
[21] H. A. Macleod, "Thin-Film Optical Filters" (2nd edition), (McGraw-Hill, New York, 1989).

David A. B. Miller (M'84–SM'89) received a B.Sc. in physics from St. Andrews University, and performed his graduate studies at Heriot-Watt University, where he was a Carnegie Research Scholar. After receiving the Ph.D. degree in 1979, he continued to work at Heriot-Watt University, latterly as a lecturer in the Department of Physics.

He moved to AT&T Bell Laboratories in 1981 as a member of the technical staff, and since 1987 has been a department head, currently of the Advanced Photonics Research Department. His research interests include optical switching and processing, nonlinear optics in semiconductors, and the physics of quantum-confined structures.

He is a senior member of the IEEE, and is a fellow of the Optical Society of America and of the American Physical Society.